

## The Effect of Point Mutations on the Free Energy of Transmembrane $\alpha$ -Helix Dimerization

Karen G. Fleming, Anne L. Ackerman and Donald M. Engelman\*

Department of Molecular  
Biophysics and Biochemistry  
Yale University, 266 Whitney  
Avenue, PO Box 208114  
New Haven, CT 06520-8114  
USA

Glycophorin A forms homodimers through interaction of the single, helical transmembrane domains of the monomers. The dimers are stable in sodium dodecylsulfate (SDS), permitting a number of studies that have identified a critical motif of residues that mediates dimer formation. We have used analytical ultracentrifugation to measure the energy of dimerization in a non-denaturing detergent solution and have observed the changes in energy arising from two of the mutants previously studied. Use of the detergent pentaoxyethylene octyl ether ( $C_8E_5$ ) is a great advantage, since its micelles are neutrally buoyant and the detergent allows a reversible association to occur between monomer and dimer states of the glycophorin A transmembrane helices during the time-scale of sedimentation equilibrium. Use of this detergent in analytical ultracentrifugation may enable a wide range of studies of molecular association events in membrane proteins.

We find that the glycophorin A transmembrane helix dimerizes with a dissociation constant of  $240(\pm 50)$  nM, corresponding to a free energy of dissociation of  $9.0(\pm 0.1)$  kcal mol<sup>-1</sup>. Point mutants that were found to be disruptive in SDS (L75A, I76A) reduced the dimer affinity in the  $C_8E_5$  detergent environment ( $K_d = 1.7(\pm 0.2)$   $\mu$ M and  $4.2(\pm 0.9)$   $\mu$ M, respectively). Thus, the earlier findings are placed on a quantitative, relative energy scale of association by our measurements. Molecular modeling and simulations suggest that the energy differences can be accounted for as changes in van der Waals interactions between helices.

© 1997 Academic Press Limited

**Keywords:** two-stage model; membrane protein; glycophorin A; ultracentrifugation;  $C_8E_5$

\*Corresponding author

### Introduction

Thermodynamically, the folding of helical membrane proteins can be considered as a two-stage process (Engelman & Steitz, 1981; Popot & Engelman, 1990). In the first stage, polypeptide segments of hydrophobic amino acid residues are established across the phospholipid bilayer as transmembrane  $\alpha$ -helices, where they may rep-

resent autonomous folding domains. Energetic considerations suggest that the insertion process can happen spontaneously and that it is driven by the hydrophobic effect. In a second stage, the formation of the  $\alpha$ -helical bundle found in the native fold of many membrane proteins occurs *via* specific side to side interactions between these already established transmembrane  $\alpha$ -helices. Factors that may drive the formation of this bundle include interchain hydrogen bonds, ion pairs, and/or packing differentials involving lipid/protein and protein/contacts.

A well-studied paradigm for stage II of membrane protein folding is the self-association of the glycophorin A transmembrane  $\alpha$ -helices that gives rise to the native dimer found in erythrocyte membranes (Bormann *et al.*, 1989; Furthmayr & Marchesi, 1976). The sequence determinants of the side to side interactions driving this second stage in the folding of glycophorin A were elucidated by an extensive mutagenesis study (Lemmon *et al.*,

Abbreviations used:  $C_8E_5$ , pentaoxyethylene octyl ether,  $C_{12}E_8$ , octyloxyethylene dodecyl ether; SN, staphylococcal nuclease; GpA, glycophorin A; SN/GpATM, the chimeric protein of SN and the transmembrane domain of GpA; SN/GpATM(L75A), SN/GpATM with leucine at GpA position 75 mutated to alanine; SN/GpATM(I76A), SN/GpATM with isoleucine at GpA position 76 mutated to alanine; PQMS, piecewise quartic molecular surface; OS, occluded surface;  $K_d$ , equilibrium dissociation constant;  $\Delta G_d^0$ , Gibbs standard free energy of dissociation.

1992a,b). Using an SDS-PAGE assay, the authors identified a motif of critical residues along one face of the transmembrane  $\alpha$ -helix and showed that even subtle mutations at specific positions in this motif could completely abrogate dimerization (Lemmon *et al.*, 1992b, 1994). Guided by this large body of biochemical data, computational approaches were used to generate a model structure comprised of a right-handed dimer of helices where the interacting helix face is formed by the residues that were found to be sensitive to mutation (Adams *et al.*, 1996; Treutlein *et al.*, 1992). The combination of the mutagenesis and computational approaches applied towards the goal of understanding membrane protein structure at high resolution has recently been validated using NMR to determine the structure of the glycoporphin A transmembrane dimer in dodecylphosphocholine micelles (MacKenzie, 1996; MacKenzie *et al.*, 1997). The NMR structure is in good agreement with the most recent computational modeling (Adams *et al.*, 1996).

The extensive mutagenesis study probing the specificity of the glycoporphin A transmembrane  $\alpha$ -helix dimerization was conducted in the classically "denaturing" environment of SDS detergent solutions. Since the glycoporphin A helix dimers are stable in SDS, these conditions were optimal for the screening of a large number of disruptive point mutations by SDS-PAGE. Although the structural determinants of the associating interface were correctly elucidated as borne out by the NMR structure, the SDS-PAGE assay did not permit measurement of the dimerization thermodynamics. In order to understand the glycoporphin A transmembrane  $\alpha$ -helix dimerization under more "native-like" conditions as well as to examine quantitatively the effect of sequence mutation on self-association, we have developed a protocol to measure the reversible association of these transmembrane  $\alpha$ -helices using analytical ultracentrifugation in the non-denaturing detergent pentaoxyethylene octyl ether ( $C_8E_5$ ).

## Results and Discussion

### The glycoporphin A transmembrane $\alpha$ -helix dimerizes with high affinity in $C_8E_5$

Sedimentation equilibrium analytical ultracentrifugation was used to measure the dimerization mediated by the glycoporphin A transmembrane  $\alpha$ -helix as fusion protein with staphylococcal nuclease (SN). There are several reasons for studying the SN/GpATM fusion protein as opposed to just the transmembrane peptide. First, the fusion protein is expressed in high yields in *Escherichia coli*, and subsequent purification is facilitated by the nuclease portion of the chimera. This expression strategy enables the preparation of a large number of fusion proteins with mutant glycoporphin A transmembrane  $\alpha$ -helices. Second, the fusion protein has a larger molar extinction coefficient than the pep-

tide alone, enabling us to access lower concentrations using absorbance optics. Finally, the chimera has a larger monomer weight, and optimal sedimentation equilibrium distributions would therefore not require extreme speeds in the ultracentrifuge. In order to eliminate the possibility that the SN portion of the fusion protein contributed to any observed association, control sedimentation equilibrium experiments were conducted on SN alone in the same buffer conditions containing detergent as was used for the fusion protein. It was found to be monomeric at the concentrations of interest (data not shown).

The equilibrium of any self association reaction in the ultracentrifuge can be measured only if the associating molecule behaves as a single thermodynamic component. Sedimentation equilibrium as well as reversibility of the association reaction on the time-scale of the experiment must be demonstrated for this to be the case. Both transport and chemical equilibrium are established when there is no longer any net transport of molecules in solution. This criterion is experimentally determined by subtracting successive absorbance *versus* radius scans collected at different times until there is no systematic difference between the two scans. Unless a sample is unstable for the long periods normally required for the equilibrium ultracentrifugation experiment, sedimentation equilibrium usually can be attained within 16 to 28 hours. While attainment of equilibrium are demonstrated in this way, the reversibility of the association reaction is demonstrated if sedimentation equilibrium data collected at different initial concentrations and speeds are well described by a global equilibrium constant (Jonhson *et al.*, 1981; Roark & Yphantis, 1969). Once sedimentation equilibrium has been achieved, it is possible to describe the oligomeric state(s) experienced by the molecules in solution. However, it is not valid to establish the relationship between these oligomers, i.e. the equilibrium constant, unless they appear to behave as a single thermodynamic component as demonstrated by reversibility.

In the special case of membrane proteins which, by their nature, require detergent micelles or phospholipid vesicles for solubilization, reversibility of the protein association reaction requires reversible association of the protein with itself (as for soluble proteins), but may also require reversibility of protein/solvent (the detergent or lipid) and solvent/solvent interactions. Further, reversibility of all three of these interactions must be kinetically possible on the time-scale of the ultracentrifugation experiment, since the protein concentration gradient is not pre-formed, but is established during centrifugation. If any one of these interactions is not reversible, the associating membrane protein may not be able to redistribute itself as a single thermodynamic component during the time-scale at which sedimentation equilibrium can be experimentally detected. Such a situation will result in

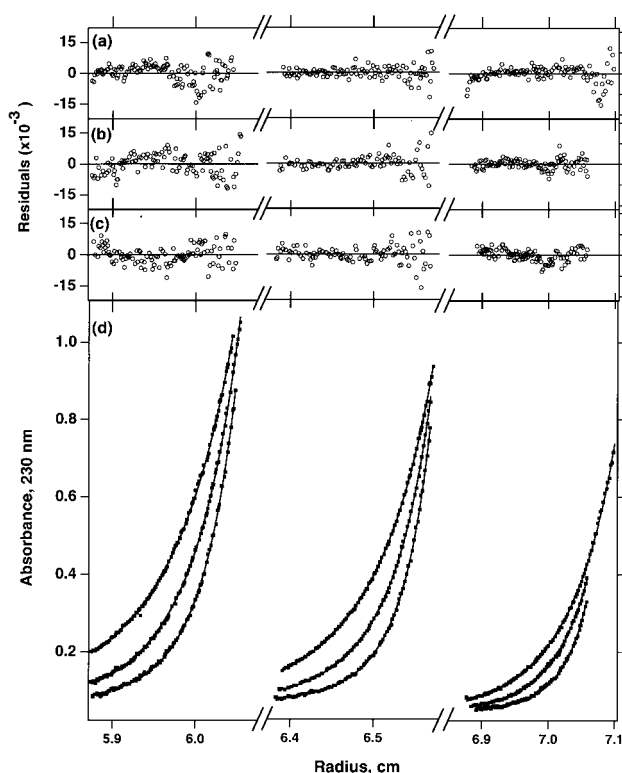


**Figure 1.** Sedimentation equilibrium distribution of SN/GpATM in 10 mM  $C_8E_5$ . (d) The equilibrium distribution data for the wt SN/GpATM at three initial concentrations ranging from 6.30  $\mu$ M to 1.97  $\mu$ M (grouped left to right) and for three speeds, 20,000, 24,500 and 30,000 rpm (left to right in each group). The squares are the data points, and the lines represent the best fit described by the global analysis of all nine data sets. The residuals of the fit are shown in the upper three panels with the concentrations arranged from left to right (high to low). (a), (b) and (c) The residuals for the 20,000, 24,500 and 30,000 rpm data sets, respectively.

a thermodynamically heterogeneous mixture of oligomers.

We first tried to measure the SN/GpATM dimerization equilibrium in  $C_{12}E_8$ , a non-denaturing detergent that has a long history of use in the ultracentrifuge for molecular mass determinations of membrane proteins (Musatov & Robinson, 1994; Reynolds & McCaslin, 1984; Reynolds & Tanford, 1976). The data could be described well by model containing monomer, dimer and tetramer terms; thus we were able to establish the oligomeric states of the SN/GpATM in  $C_{12}E_8$ . However, global data analysis attempts were unsuccessful, suggesting that the association reaction was not reversible on the time-scale of the experiment. The observed  $K_d$  for dimer formation ranged from nanomolar to tens of micromolar, and the estimated parameter values were not repeated by successive experimental setups (data not shown). The association reaction's failure to demonstrate reversibility was always true in detergent solutions containing

$C_{12}E_8$ , even when extended periods of centrifugation were carried out in order to allow for the possibility of slow reversibility (e.g. experiments at 37°C for seven days per speed).

We then tried measurements in  $C_8E_5$ , a chemically similar, also non-denaturing detergent. A major difference between these two detergents is that  $C_8E_5$  has a much higher critical micelle concentration, perhaps resulting in a more kinetically dynamic solvent environment. In contrast to  $C_{12}E_8$ , we were able to attain sedimentation equilibrium as well as demonstrate reversibility of SN/GpATM dimerization in  $C_8E_5$  detergent solutions. The concentration versus radial distance profiles for SN/GpATM in 10 mM  $C_8E_5$  at three speeds and three concentrations are shown in Figure 1. The statistics for the sedimentation equilibrium fits are detailed in Table 1. The results of the data analysis revealed a monomer/dimer/tetramer distribution in  $C_8E_5$ , where the SN/GpATM dimer was found to be the predominant species in solution.

The distribution of species and the monomer/dimer equilibrium constant were determined by global non-linear least-squares analysis of the nine data sets. This was accomplished by starting with the simplest model (single, ideal) and then considering models of increasing complexity until the residuals became random and the variance was minimized. A plot of the natural logarithm of the protein concentration versus the square of the radius for each of the data sets individually showed upward curvature, indicative of more than one species in solution (data not shown), eliminating a single-species model. Further, the data were found to be poorly described by either a simple monomer-dimer or monomer-trimer model, and in no case did inclusion of a non-ideality parameter significantly improve the fits. Assuming that the contribution of any bound detergent is zero (see Materials and Methods), the best fit to the data was an ideal monomer-dimer-incompetent tetramer model (equation (1)):

$$c_i = c_{\text{ref}} \exp \left[ \sigma_1 \left( \frac{r_i^2}{2} - \frac{r_{\text{ref}}^2}{2} \right) \right] + \frac{c_{\text{ref}}^2}{K_{2,1}} \exp \left[ 2\sigma_1 \left( \frac{r_i^2}{2} - \frac{r_{\text{ref}}^2}{2} \right) \right] + \frac{c_{\text{ref}}^4}{K_{4,1}^*} \exp \left[ 4\sigma_1 \left( \frac{r_i^2}{2} - \frac{r_{\text{ref}}^2}{2} \right) \right] + \delta \quad (1)$$

where  $c_i$  is the total absorbance at a radial position,  $r_i$ ;  $c_{\text{ref}}$  is a monomer absorbance at a reference position,  $r_{\text{ref}}$ ;  $\sigma_1 = M(1 - \bar{v}_{\text{Pr}}\rho)\omega^2/RT$ ;  $M$  is the monomer molecular mass (21,223);  $\bar{v}_{\text{Pr}}$  is the monomer partial specific volume (calculated as 0.7476 ml g<sup>-1</sup>);  $\rho$  is the solvent density (calculated as 1.0075 g ml<sup>-1</sup>);  $\omega$  is the angular velocity (radians second<sup>-1</sup>);  $R$  is the universal gas constant;  $T$  is the absolute temperature;  $\delta$  is a baseline term for non-sedimenting material;  $K_{2,1}$  is the apparent monomer-dimer dissociation constant (in absorbance units) that was

**Table 1.** Summary of sedimentation equilibrium analysis of glycoporphin proteins in  $C_8E_5$ 

Conditions	Protein	$K_d^a$ ( $\mu$ M)	$\Delta G_d$ (kcal mol <sup>-1</sup> )	$\Delta(\Delta G_d)$ (kcal mol <sup>-1</sup> )	SRV <sup>b</sup> ( $\times 10^{-3}$ )	DOF <sup>c</sup>
10 mM $C_8E_5$	wt	0.22 $\pm$ 0.07	9.1 $\pm$ 0.2	NA	4.26	899
	L75A	1.6 $\pm$ 0.1	7.9 $\pm$ 0.1	1.2 $\pm$ 0.2	6.28	927
33 mM $C_8E_5$	wt	0.24 $\pm$ 0.05	9.0 $\pm$ 0.1	NA	5.42	1097
	L75A	1.7 $\pm$ 0.2	7.9 $\pm$ 0.1	1.1 $\pm$ 0.1	4.79	1109
	I76A	4.2 $\pm$ 0.9	7.3 $\pm$ 0.1	1.7 $\pm$ 0.1	7.41	1004

<sup>a</sup> The  $K_d$  values correspond to the common monomer-dimer equilibrium constants determined in a global fit of the data to a monomer-dimer-incompetent tetramer model as described in the text. The individually observed tetramer dissociation constants are not detailed, but were found to range from tens to hundreds of micromolar for all three proteins. The error listed for each parameter represents the 67% confidence interval from the fit, or, for the free energies, the propagated error (Bevington, 1969).

<sup>b</sup> The SRV is the square-root of the variance reported by the MacNONLIN algorithm.

<sup>c</sup> The DOF are the degrees of freedom for each fit, which is the difference between the total number of data points and the number of fitted parameters.

found to be common to all data sets; and  $K_{4,1}^*$  is the apparent monomer-tetramer dissociation constant (in absorbance units) that was individually estimated for each data set. Since the monomer-dimer equilibrium dissociation constant could be well described by a single parameter for all data sets, the analysis indicates that the monomeric and dimeric species are indeed reversibly associating during the time-scale of sedimentation equilibrium. When converted to molar units, the equilibrium dissociation constant in 10 mM  $C_8E_5$  was found to be 220 nM with 67% upper and lower confidence limits of 290 nM and 150 nM, respectively. At 25°C these values correspond to a  $\Delta G_d$  of 9.1( $\pm$ 0.2) kcal mol<sup>-1</sup>.

The presence of a tetrameric species both in  $C_{12}E_8$  and in  $C_8E_5$  solutions was somewhat surprising, since it had not been observed using the SDS-PAGE assay. It is not an artifact of the fitting procedure, since we could subsequently verify its existence in the centrifuge samples by covalent cross-linking following sedimentation analysis. SDS-PAGE of cross-linked samples showed the presence of a specific higher-order species migrating at an apparent molecular mass corresponding to that of a tetramer (data not shown). The fact that we observed distinct  $K_{4,1}^*$  values for the tetramer in different data sets suggests that it is a thermodynamically heterogeneous species. The concentration trend of the individually estimated  $K_{4,1}^*$  values was generally found to be decreasing with decreasing protein concentration: a trend that is diagnostic of a tetrameric species that is unable to dissociate upon dilution and is thus termed incompetent. The amount of sample is found as incompetent tetramer as described by the best fit model above was less than 10% of the total except for two data sets, where it was 13%. Additional models containing three species were tested in order to verify that the current model was the best description of the data. As evidenced by non-randomness of the residuals as well as an increased variance for the fits, the data were not well described by either a monomer-dimer-tetramer model in which the tetramer would be in equilibrium with the other species or by a model in which the dimer species would be considered in-

competent and the monomer and tetramer species would be in equilibrium with each other.

### The dimerization is independent of micelle concentration

The forces that drive association of membrane proteins in the detergent environment must involve not only protein-protein interactions, but also protein-detergent and detergent-detergent interactions. Since the detergent is essentially the solvent for the interacting segment of this membrane protein, it is reasonable to postulate that the detergent to protein ratio could be a major determinant in driving the self-association. In the case where micelles are limiting, Tanford & Reynolds (1976) have proposed that associated species may arise due to "artificial togetherness"; a condition in which the equilibrium mixture contains more than one polypeptide chain per micelle in the absence of any attractive forces between them. They further propose that dilution of protein-detergent particles with excess detergent micelles until a constant molecular mass (or a constant equilibrium constant) is obtained should overcome the problem of artificial togetherness and yield an oligomeric state that should correspond to that found under native conditions, as long as the detergent stimulates the native environment in the membrane (Tanford & Reynolds, 1976). In order to ensure that the dimerization constant measured by ultracentrifugation actually reflects the attractive forces present between GpA transmembrane helices and to eliminate artificial togetherness as an explanation for the observed dimerization, we conducted experiments at two detergent concentrations where the total micelle concentration varied by fivefold. As measured in the ultracentrifuge, if artificial togetherness was driving the observed association, increasing the micelle concentration fivefold would be reflected in a fivefold increase in the apparent dissociation constant as measured in molar units. A difference of this magnitude could certainly be measured with high confidence in our system.

Global analysis of sedimentation equilibrium data revealed that the wild-type dimerization dissociation constant in 33 mM  $C_8E_5$  (approximately

316  $\mu\text{M}$  micelles) was  $240(\pm 50)$  nM. This value is within error of that found in 10 mM  $\text{C}_8\text{E}_5$  (approximately 63  $\mu\text{M}$  micelles). The observation that the dissociation constant is invariant with detergent to protein ratio suggests that the micelle solvent is not limiting and is not the major driving force in the observed helix-helix association under our conditions in  $\text{C}_8\text{E}_5$ . A common dissociation constant in different detergent concentrations was also observed for the point mutant SN/GpATM(L75A) (see Table 1).

### Disruptive point mutations at interface positions result in decreased dimerization

The dimerization of two point mutants of the SN/GpATM transmembrane  $\alpha$ -helix was also measured. The substitution of alanine for leucine at position 75 is scored in the SDS-PAGE assay as predominantly monomer with detectable dimer (Lemmon *et al.*, 1992b). Figure 2(a) shows the exponential distribution of three of the data sets used in the global analysis of the SN/GpATM(L75A) point mutant in 33 mM  $\text{C}_8\text{E}_5$ . The global analysis revealed that the equilibrium dissociation constant for dimer formation at 25°C was  $1.7(\pm 0.2)$   $\mu\text{M}$ , an

increase of approximately sixfold as compared to the wild-type; resulting in a decreased free energy of dissociation,  $\Delta(\Delta G_d)$ , of  $1.1(\pm 0.1)$  kcal mol<sup>-1</sup>. Experiments on this mutant were also done in 10 mM  $\text{C}_8\text{E}_5$ , where the equilibrium dissociation constant was found to be  $1.6(\pm 0.1)$   $\mu\text{M}$ . As with the wild-type protein, this dissociation is within error of that determined in 33 mM  $\text{C}_8\text{E}_5$ , supporting the notion that the hydrophobic solvent is not limiting under our experimental conditions.

The substitution of alanine for isoleucine at position 76 scored in the SDS-PAGE assay as abolishing dimer formation. Figure 2(b) shows the exponential distribution of three of the data sets used in global analysis of the SN/GpATM(I76A) point mutant. The global analysis revealed that the equilibrium dissociation constant for dimer formation was  $4.2(\pm 0.9)$   $\mu\text{M}$ , an increase of approximately 19-fold as compared to the wild-type transmembrane domain; resulting in a decreased free energy of dissociation of  $1.7(\pm 0.1)$  kcal mol<sup>-1</sup>. As in the case of the wild-type protein, the global description of the equilibrium data for both mutants required a model that contained an incompetent tetramer species in addition to the observed

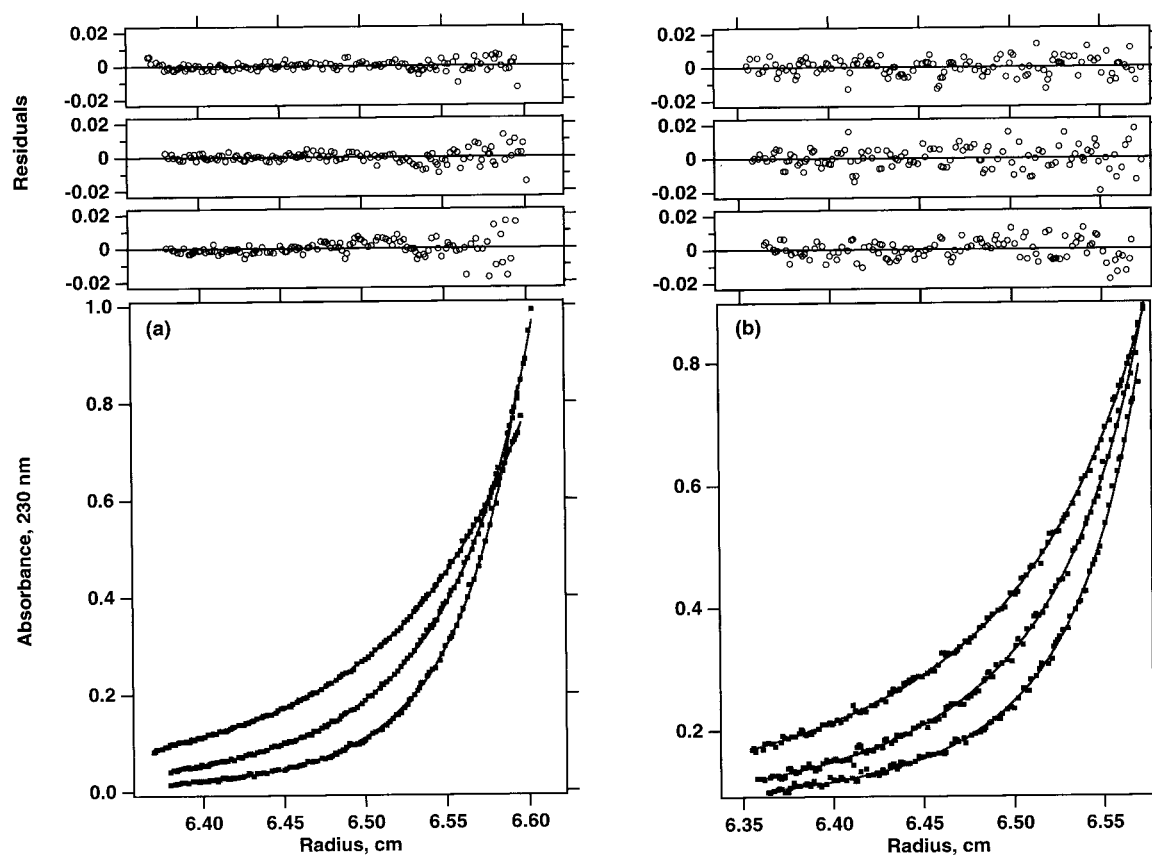


**Figure 2.** Sedimentation equilibrium distribution of mutant transmembrane proteins. (a) and (b) The equilibrium distribution data for SN/GpATM(L75A) and SN/GpATM(I76A), respectively. Data are shown for a single concentration and rotor speeds of 20,000, 24,500 and 30,000 rpm. The squares are the data points, and the lines are the best fits described by the global analysis of nine data sets each. The residuals for each protein are shown in the three panels above the each data set and are arranged from 20,000 (top) to 30,000 rpm (bottom).

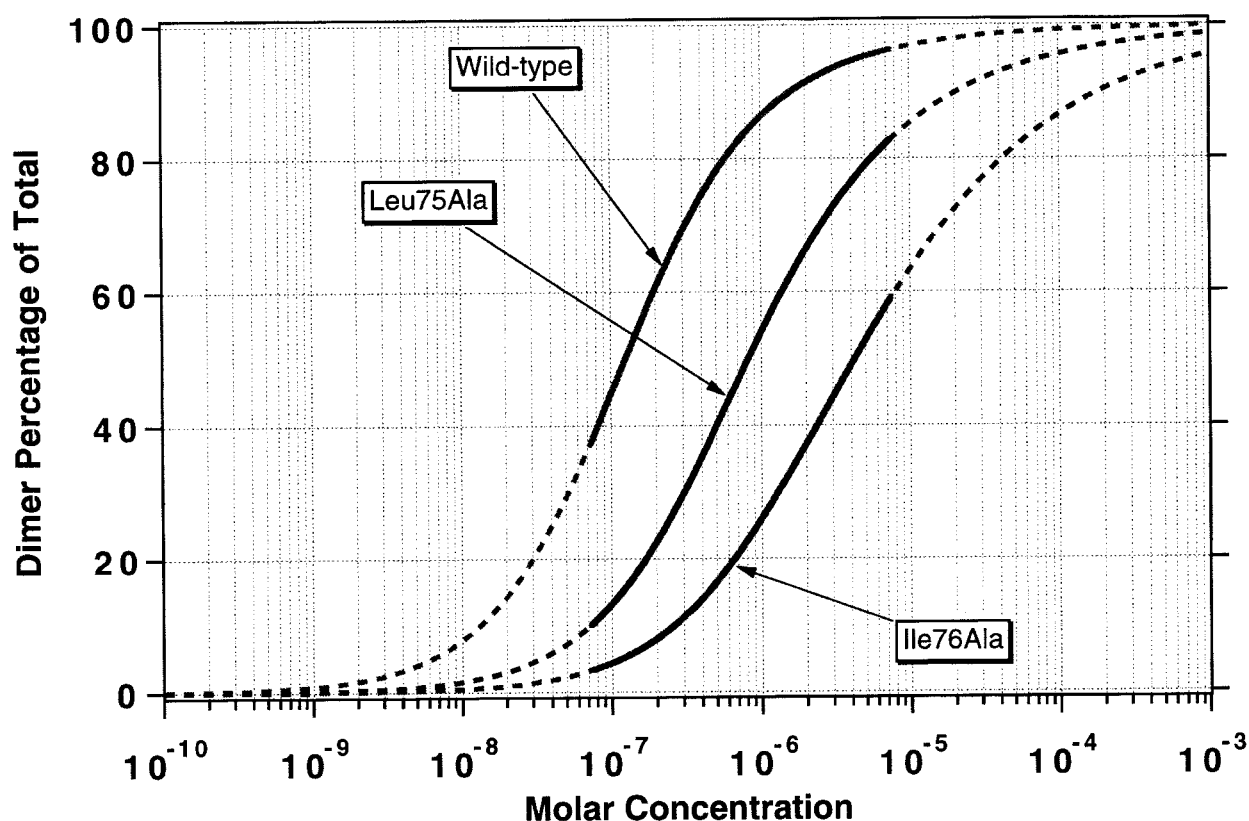


**Figure 3.** Distribution of dimeric transmembrane proteins in  $C_8E_5$  as a function of total concentration. The estimated dimerization dissociation constants from ultracentrifugation were used to generate the distribution of the equilibrium monomer and dimer species as a function of total concentration. The continuous portions of the curves indicate the concentration range wherein the analysis was carried out. The broken portions of the curves are extrapolated from analysis of those data. The distributions were calculated assuming excess detergent solvent at all protein concentrations. For clarity, only the dimeric species for each transmembrane protein is shown; the remainder of the total species in solution would be the monomer.

equilibrium monomer and dimer species. The amount of incompetent tetramer in the mutant samples was also 10% or less.

#### The detergent environment causes a shift in the interaction energy scale

Although the dissociation constants for both the wild-type and L75A proteins are independent of micelle concentration in  $C_8E_5$ , the observation of larger amounts of dimer in the mutant proteins in this study compared with the SDS-PAGE assay reported by Lemmon *et al.* (1992b) suggests that the energy scale of interactions is shifted in  $C_8E_5$ . The concentration-dependence of dimer formation measured in  $C_8E_5$ , is plotted in Figure 3, where the relative percentages of the dimer are shown for all three chimeric SN/GpATM proteins. Assuming excess detergent solvent conditions at all protein concentrations, the distributions were computed using the observed dissociation constants and then extrapolated over a wide concentration range. At the concentration range at which the SDS solution studies were done (10 to 30  $\mu$ M), both mutants show significant amounts of dimer in  $C_8E_5$ . The rank

order of disruption, however, remains identical with that observed in SDS. Thus, the data suggest that only the overall scale of interactions is shifted towards a more associated form in  $C_8E_5$ .

Other studies also indicate that there is a greater proportion of GpA transmembrane dimer present in mutant proteins when the subunit composition is analyzed in more "native-like" environments as compared to SDS (Adair, 1993; Langosch *et al.*, 1996). Most recently, dimerization of the glycoporphin A helix as a fusion protein with the ToxR transcription activator in bacterial membranes has been reported (Langosch *et al.*, 1996). By alanine scanning mutagenesis, the authors confirmed that at least four of the residues (I76, G79, G83 and T87) from the GpA dimerization motif are critical for dimer formation. In general though, the authors found that the transmembrane dimerization in bacterial membranes appears to be less sensitive to mutation than would be indicated by the mutagenesis study conducted in SDS or by the present study in  $C_8E_5$ . For example, the dimerization of the leucine 75 to alanine mutant in their study was found to be not significantly different from that of wild-type. The authors estimate that the concen-

tration of the ToxR-GpATM fusion proteins in the bacterial inner membrane is of the order of 1 mM and propose that the high local concentration as well as preorientation in membranes strongly favors dimer formation in membranes. Both of these factors could contribute to the diminished sensitivity of their assay to the sequence-dependence of the GpATM dimerization. Even ultracentrifugation would be unable to distinguish between these mutants if it were conducted at millimolar concentrations. It may be that the entire motif defined by Lemmon *et al.* (1992b) is indeed critical for dimer formation in bacterial membranes when the concentration of expressed protein is at a level low enough that the differences in dimerization propensity can be observed.

### The decreased dimerization propensity for L75A and I76A can be explained by decreased packing at the dimer interface

It has been proposed that the decrease in protein stability associated with a leucine to alanine replacement in the core of soluble proteins consists of two energy terms (Eriksson *et al.*, 1992; Mathews, 1993). The first term is a constant energy term related to the difference in hydrophobicity between leucine and alanine as estimated by their relative transfer free energies. When considered within the context of the two-stage model of membrane protein folding, hydrophobicity would not be expected to play a role on helix-helix association (stage II), since it is already taken into account in the establishment of the transmembrane helices themselves (stage I: Engelman & Steitz, 1981). Energetic considerations suggest that the non-polar transbilayer helix is so stable that it can even accommodate several polar groups. Thus, the difference in the hydrophobicity between leucine and alanine should affect neither the stability of the transmembrane helix nor its subsequent self-association. The second energy term proposed by Eriksson *et al.* (1992) is associated with the increase in cavity size that occurs when a larger side-chain (leucine) is replaced by a smaller one (alanine), as estimated by calculating the increase in cavity surface area. The physical basis for this cavity-dependent energy term can be rationalized in terms of a decrease in the buried molecular surface area in-

involved in van der Waals contacts in the mutated protein. An energy cost of  $20 \text{ cal mol}^{-1} \text{ \AA}^{-2}$  has been suggested.

A common theme that emerges from the mutagenesis and NMR studies on the glycoporphin A transmembrane domain is that the observed specificity driving the dimerization arises from van der Waals interactions. We performed molecular modeling and simulations of the mutant glycoporphin A helical dimers in order to generate coordinates of model structures. These structures were then analyzed as described below to determine if reduced packing of the dimer interface, as expressed in a decrease in interchain buried molecular surface area, could account for the decreased free energy of dissociation observed for the glycoporphin A dimers. We first considered the interchain buried molecular surface area of these model structures using the PQMS algorithm (Connolly, 1985). The results of the calculations are shown in Table 2. The interchain buried molecular surface area was decreased in the mutant dimers as compared to the wild-type dimer. The PQMS calculations showed a decrease of  $80(\pm 7)$  and  $79(\pm 11) \text{ \AA}^2$  in the interchain buried molecular surface area for the L75A and I76A mutants, respectively. Using the value of  $20 \text{ cal mol}^{-1} \text{ \AA}^{-2}$  these decreases would correspond to a free energy of destabilization of approximately  $1.6 \text{ kcal mol}^{-1}$ : a predicted value not far from the experimentally observed free energy differences for these mutants as compared to the wild-type. This method, however, does not explain the observed differences in the dimerization propensities between the two mutants. One possible reason may be that the molecular surface area calculated in this manner is not sensitive to packing defects that are too small to be detected by this spherical probe method.

We then used an extension of the occluded surface (OS) algorithm to evaluate the interchain occluded molecular surface area of model dimers (Pattabiraman *et al.*, 1995). The occluded molecular surface is related to, but distinct from the buried molecular surface in that it represents that portion of the molecular surface of an atom that is occluded by its surrounding atoms. It can be thought of as a degree of atomic interaction and interpreted as an estimate of packing. The OS analysis of model glycoporphin A dimers revealed a decrease in the interchain occluded molecular surface area for the mutants as compared to the wild-type structures (see Table 2). In addition, OS was further able to distinguish between the two mutants. As compared to the wild-type, the decrease in the interchain occluded molecular surface area observed for the L75A mutant was  $58(\pm 9) \text{ \AA}^2$  whereas a decrease of  $80(\pm 9) \text{ \AA}^2$  was calculated for the I76A mutant. If the energetic penalty of  $20 \text{ cal mol}^{-1} \text{ \AA}^{-2}$  per increase in non-interfacing surface area is applied here, the decreases in occluded molecular surface area would correspond to decreases in free energies of dissociation of  $1.2(\pm 0.2)$  and  $1.6(\pm 0.2) \text{ kcal mol}^{-1}$ , respectively.

**Table 2.** Interface packing calculations on model glycoporphin A dimers

Protein	Buried Molecular surface ( $\text{\AA}^2$ )	Occluded Molecular surface ( $\text{\AA}^2$ )
Wild-type	$587 \pm 6$	$560 \pm 7$
L75A	$507 \pm 4$	$502 \pm 6$
$\Delta(\text{L75A-wt})$	$-80 \pm 7$	$-58 \pm 9$
I76A	$508 \pm 10$	$480 \pm 6$
$\Delta(\text{I76A-wt})$	$-79 \pm 11$	$-80 \pm 9$

The values shown are the mean and standard deviations of the surface areas for the ensemble of the 100 model structures.

These values agree remarkably well with the  $\Delta(\Delta G_d)$  values measured in the ultracentrifuge, supporting the hypothesis that destabilization of the dimer by mutation at these sensitive residues can be explained by decreased van der Waals interactions at the dimer interface.

## Conclusion

The ability to measure a reversible association reaction using sedimentation equilibrium in detergent solutions of  $C_8E_5$  is a major attraction for its use in studies of membrane protein association.  $C_8E_5$  also provides a mild, minimally denaturing environment in which to evaluate membrane protein oligomerization properties. Ideally, thermodynamic studies would be conducted in phospholipid vesicles or in membranes; however, the requirement of a kinetically accessible reversible association during the time-scale of sedimentation equilibrium precludes the measurement of transmembrane helix-helix energetics in those environments. Even if the absolute energies found in  $C_8E_5$  do not translate directly to those observed in membranes, this protocol still affords a highly sensitive and quantitative method for measuring the effect of sequence mutation relative to a standard while keeping all other variables constant. Thus, although the scale may be shifted, the  $\Delta(\Delta G_d)$  values will be informative and will allow us to begin to understand the portion of the energy term in membrane protein associations that arises from the protein-protein interactions of helical transmembrane segments. Combined with computational modeling and in some cases high-resolution structural approaches  $\Delta(\Delta G_d)$  measurements of this type should help to guide our understanding of the chemistry of interactions within helical membrane proteins in hydrophobic environments. Once a database for the quantitative correlation of mutations on membrane protein interactions has been established, this knowledge will be useful in prediction and in protein design.

## Materials and Methods

### Sample preparation

The construction, expression and purification of the staphylococcal nuclease/glycophorin A transmembrane domain fusion protein (SN/GpATM) has been described in detail (Lemmon *et al.*, 1992a). The construction of plasmids encoding the mutant proteins SN/GpATM(L75A) and SN/GpATM(I76A) has been described (Lemmon *et al.*, 1992b). These proteins were purified using the same protocol as for the wild-type protein. All proteins were purified in the detergent Thesit<sup>®</sup>. Detergent exchange into  $C_8E_5$  was accomplished by binding proteins in Thesit<sup>®</sup> to a cation-exchange column, washing with a minimum volume of ten column volumes of buffer containing  $C_8E_5$ , followed by elution with high salt in  $C_8E_5$ . Before ultracentrifugation experiments all samples were

diluted with centrifugation buffer that contained 20 mM sodium phosphate (pH 7.0), 200 mM sodium chloride supplemented with the desired concentration of  $C_8E_5$ . Samples were dialyzed for a minimum of 24 hours against the same buffer.

### Analytical ultracentrifugation

Sedimentation equilibrium analytical ultracentrifugation was performed with Beckman Optima XL-I ultracentrifuge using the absorbance optics system to visualize the protein at 230 nm. Six-sector cells were used, and data were acquired every 0.001 cm with ten replicates. Sample volumes were 110  $\mu$ l. Data were collected at 25°C at speeds of 20,000, 24,500 and 30,000 revolutions per minute. In all cases data were collected at a minimum of three initial protein concentrations that ranged from 1 to 7  $\mu$ M. Absorbance *versus* radius scans were collected at 120 minute intervals, and successive scans were compared graphically using the XL-I software to ensure that the sample reached sedimentation equilibrium. The protein partial specific volumes were calculated from the amino acid composition using the values reported by Cohn & Edsall (1943). The solvent density was estimated by summing the density increments of the buffer components as described by Laue *et al.* (1992).  $C_8E_5$  was obtained from sigma at >99% purity, which was subsequently confirmed by electrospray mass spectrometry. The micelle partial specific volume is reported to be approximately 0.993  $\text{cm}^3 \text{g}^{-1}$  (Ludwig *et al.*, 1982).

Global analysis of sedimentation equilibrium data was accomplished using the Macintosh version of the NON-LIN algorithm (Johnson *et al.*, 1981). A minimum of the nine data sets collected at multiple concentrations and speeds was used in the estimation of parameters. The value of  $\sigma_1$  was fixed to correspond to the calculated buoyant molecular mass of the monomer assuming that the contribution of any bound detergent was zero (see below). Goodness of fit was determined by examination of the residuals and minimization of the variance. Apparent absorbance equilibrium constants were converted to molar units using a molar extinction coefficient of the SN/GpATM proteins of 126,977 at 230 nm (McRorie & Voelker, 1993).

Since these proteins are in complex with detergent, the buoyant molecular mass of the sedimenting particle,  $M_{Pr}(1 - \phi' \rho)$  contains contributions from both the protein and the bound detergent. In order to account for these separate contributions, the buoyant molecular mass of the complex can be rewritten in terms of its components (Cassassa & Eisenberg, 1964; Reynolds & Tanford, 1976):

$$M_{Pr}(1 - \phi' \rho) = M_{Pr}[(1 - \bar{v}_{Pr}\rho) + \delta_{Det}(1 - \bar{v}_{Det}\rho)]$$

where  $\bar{v}_{Pr}$  and  $\bar{v}_{Det}$  are the partial specific volumes of the protein and detergent, respectively;  $\delta_{Det}$  is the amount of detergent bound in grams per gram of protein, and  $\rho$  is the solvent density. In the case of  $C_8E_5$ , the product of  $\bar{v}_{Det}\rho$  is 0.999, thus it is not necessary to know the value of  $\delta_{Det}$ . Even if the value for  $\delta_{Det}$  is as high as 2 g/g monomer, the term  $\delta_{Det}(1 - \bar{v}_{Det}\rho)$  is equal to 0.002, which would introduce an error of less than 1% in the monomer buoyant molecular mass, a value much lower than the precision typically observed in sedimentation equilibrium experiments. The analysis of this multicomponent system then becomes pseudo-two component and  $M_{Pr}(1 - \phi' \rho)$  essentially equal to  $M_{Pr}(1 - \bar{v}_{Pr}\rho)$ .

### Molecular modeling and simulation calculations

Models for the point mutants considered in this study were generated from a set of the NMR coordinates using the molecular graphics program TurboFrodo version 5.5. Molecular simulations of the structure of the glycoporphin A dimer point mutants were carried out with X-PLOR following the protocol of Adams (Adams & Brünger, 1996; Brünger, 1992). The OPLS united atom topology and parameter sets were used (Jorgensen & Tirado-Rives, 1988; Tirado-Rives & Jorgensen, 1990) with all polar and aromatic hydrogen atoms included. Briefly, a protocol employing 1000 steps (1 ps total) of molecular dynamics was found to be sufficient to reach equilibrium. Initial velocities came from a Maxwell distribution. This was followed by 200 steps of minimization. Simulations were carried out *in vacuo* at a constant temperature of 300 K by coupling to a heat bath (Berendsen *et al.*, 1984). Only the helical domain of the NMR structure (residues 70 through 91) was considered in the calculations, and only those amino acid side-chains in van der Waals contact with either leucine 75 or isoleucine 76 (as well as the mutated position itself) were unrestrained during the simulations; all other residues were harmonically restrained (force constant = 25 kcal mol<sup>-1</sup> Å<sup>-2</sup>) to their original coordinates. Half-sided distance restraints were applied between O<sub>i</sub> and N<sub>i+4</sub> in order to maintain an  $\alpha$ -helical conformation in the unrestrained residues. The wild-type sequence was subjected to the same simulations as a control.

Analysis of atomic packing of 100 model structures generated by molecular dynamics was accomplished by evaluation of the interchain buried molecular surface using both the PQMS algorithm of Connolly (1985) and the OS algorithm of Pattabiraman *et al.* (1995). The interchain buried molecular surface area was calculated using the PQMS algorithm employing a probe size of 1.2 Å so that the results would be directly comparable to the molecular surface calculations conducted on the lysozyme mutants by Eriksson *et al.* (1992). The molecular surface calculations were also performed employing a probe size of 1.4, 2.0 and 2.5 Å with essentially the same results. The interchain molecular surface area was determined by subtracting the molecular surface area calculated for the dimer from the sum of the molecular surface areas calculated for each monomer.

The interchain occluded surface area was calculated using an extension of the OS algorithm (Pattabiraman *et al.*, 1995). In this method, a molecular dot surface of each residue is calculated with a 1.4 Å probe using the MS program of Connolly (1985). A normal is then extended radially from each dot until it either intersects the van der Waals surface of a neighboring atom or reaches a length of 2.8 Å (the diameter of a water molecule). The occluded surface area, OS, is that molecular surface area on the originating atom associated with normals that intersect another atom as opposed to reaching the 2.8 Å limit; all other molecular surface area is considered non-occluded. The interchain occluded surface area is calculated by summing the occluded surface area for only those extended normals that were found to intersect atoms on the opposing chain.

### Acknowledgments

We are grateful to B. A. Churnyk at Pfizer Central Research (Groton, CT), who generously provided access to

their XL-A for the collection of preliminary data and made these studies possible. We thank C. B. Millard and C. A. Broomfield at the Aberdeen Proving Grounds (Edgewood, MD), and S. Hale and P. Schimmel at MIT (Boston, MA) for providing additional XL-A instrument time for the C<sub>12</sub>E<sub>8</sub> studies; G. Olack and F. M. Richards for the mass spectrometry on C<sub>8</sub>E<sub>5</sub>; Jürg P. Rosenbusch and P. D. Adams for helpful conversations; and T. M. Laue, W. F. Stafford III, P. Hensley and P. D. Adams for critically reading the manuscript. The MacNONLIN software was provided by the University of Connecticut Biotechnology Center (Storrs, CT). This work was supported by NIH grants GM16579 (to K. G. F.), GM54160 and GM22778 (to D. M. E.) and funds from the National Foundation for Cancer Research (to D. M. E.).

### References

- Adair, B. D. (1993). The influence of packing on the folding of integral membrane proteins. PhD thesis, Yale University, New Haven.
- Adams, P. D., Engelman, D. M. & Brünger, A. T. (1996). Improved prediction for the structure of the dimeric transmembrane domain of glycoporphin A obtained through global searching. *Protein Struct. Funct. Genet.* **26**, 257–261.
- Berendsen, J. J. C., Postma, J. P. M., van Gunsteren, W. F., DiNola, A. & Haak, J. R. (1984). Molecular dynamics with coupling to an external bath. *J. Chem. Phys.* **81**, 3684–3690.
- Bevington, P. R. (1969). *Data Reduction and Error Analysis for the Physical Sciences*, McGraw-Hill Book Company, New York.
- Bormann, B. J., Knowles, W. J. & Marchesi, V. T. (1989). Synthetic peptides mimic the assembly of transmembrane glycoproteins. *J. Biol. Chem.* **264**, 4033–4037.
- Brünger, A. T. (1992). *X-PLOR, Version 3.1, A System for X-ray Crystallography and NMR*, Yale University Press, New Haven, CT.
- Cassassa, E. F. & Eisenberg, H. (1964). Thermodynamic analysis of multicomponent systems. *Advan. Protein Chem.* **19**, 287–395.
- Cohn, E. J. & Edsall, J. T. (1943). Density and apparent volume of proteins. In *Proteins, Amino Acids and Peptides* (Cohn, E. J. & Edsall, J. T., eds), pp. 370–381, Reinhold Publishing Corporation, New York.
- Connolly, M. L. (1985). Computation of molecular volume. *J. Am. Chem. Soc.* **107**, 1118–1124.
- Engelman, D. M. & Steitz, T. A. (1981). The spontaneous insertion of proteins into and across membranes: the helical hairpin hypothesis. *Cell*, **23**, 411–422.
- Eriksson, A. E., Baase, W. A., Xhang, X.-J., Heinz, D. W., Blaber, M. P. B. E. & Mathews, B. W. (1992). Response of a protein structure to cavity-creating mutations and its relation to the hydrophobic effect. *Science*, **255**, 178–183.
- Furthmayr, H. & Marchesi, V. T. (1976). Subunit structure of human erythrocyte glycoporphin A. *Biochemistry*, **15**, 1137–1144.
- Johnson, M. L., Correia, J. J., Yphantis, D. A. & Halvorson, H. R. (1981). Analysis of data from the analytical ultracentrifuge by nonlinear least-squares techniques. *Biophys. J.* **36**, 575–588.
- Jorgensen, W. L. & Tirado-Rives, J. (1988). The OPLS potential functions for proteins. Energy minimizations

- for crystals of cyclic peptides and crambin. *J. Am. Chem. Soc.* **110**, 1657–1666.
- Langosch, D., Brosig, B., Kolmar, H. & Fritz, H.-J. (1996). Dimerisation of the glycoporphin A transmembrane segment in membranes probed with the ToxR transcription activator. *J. Mol. Biol.* **263**, 525–530.
- Laue, T. M., Shah, B., Ridgeway, T. M. & Pelletier, S. L. (1992). Computer-aided interpretation of analytical sedimentation data for proteins. In *Analytical Ultracentrifugation in Biochemistry and Polymer Science* (Harding, S. E., Rowe, A. J. & Horton, J. C., eds), pp. 90–125, Royal Society of Chemistry, Cambridge.
- Lemmon, M. A., Flanagan, J. M., Hunt, J. F., Adair, B. D., Bormann, B. J., Dempsey, C. E. & Engelman, D. M. (1992a). Glycophorin A dimerization is driven by specific interactions between transmembrane  $\alpha$ -helices. *J. Biol. Chem.* **267**, 7683–7689.
- Lemmon, M. A., Flanagan, J. M., Treutlein, H. R., Zhang, J. & Engelman, D. M. (1992b). Sequence specificity in the dimerization of transmembrane  $\alpha$ -helices. *Biochemistry*, **31**, 12719–12725.
- Lemmon, M. A., Treutlein, H. R., Adams, P. D., Brunger, A. T. & Engelman, D. M. (1994). A dimerization motif for transmembrane  $\alpha$ -helices. *Nature Struct. Biol.* **1**, 157–163.
- Ludwig, B., Grabo, M., Gregor, I., Lustig, A., Regenass, M. & Rosenbusch, J. P. (1982). Solubilized cytochrome c oxidase for *Paracoccus denitrificans* is a monomer. *J. Biol. Chem.* **257**, 5576–5578.
- MacKenzie, K. R. (1996). Structure determination of the dimeric membrane spanning domain of glycoporphin A in detergent micelles by triple resonance spectroscopy. PhD thesis, Yale University, New Haven.
- MacKenzie, K. R., Prestegard, J. H. & Engelman, D. M. (1997). A transmembrane helix dimer: structure and implications. *Science*, **276**, 131–133.
- Mathews, B. W. (1993). Structural and genetic analysis of protein stability. *Annu. Rev. Biochem.* **62**, 139–160.
- McRorie, D. K. & Voelker, P. J. (1993). *Self-Associating Systems in the Analytical Ultracentrifuge*, Beckman Instruments, Inc, Fullerton, CA.
- Musatov, A. & Robinson, N. C. (1994). Detergent-solubilized monomeric and dimeric cytochrome *bc*<sub>1</sub> isolated from bovine heart. *Biochemistry*, **33**, 13005–13012.
- Pattabiraman, N., Ward, K. B. & Fleming, P. J. (1995). Occluded molecular surface: analysis of protein packing. *J. Mol. Recogn.* **8**, 334–344.
- Popot, J.-L. & Engelman, D. M. (1990). Membrane protein folding and oligomerization: the two-stage model. *Biochemistry*, **29**, 4032–4037.
- Reynolds, J. A. & McCaslin, D. R. (1985). Determination of protein molecular weight in complexes with detergent without knowledge of binding. *Methods Enzymol.* **117**, 41–53.
- Reynolds, J. A. & Tanford, C. (1976). Determination of molecular weight of the protein moiety in protein-detergent complexes without direct knowledge of detergent binding. *Proc. Natl Acad. Sci. USA*, **73**, 4467–4470.
- Roark, D. E. & Yphantis, D. A. (1969). Studies of self-associating systems by equilibrium ultracentrifugation. *Ann. N.Y. Acad. Sci.* **164**, 245–278.
- Tanford, C. & Reynolds, J. A. (1976). Characterization of membrane proteins in detergent solutions. *Biochim. Biophys. Acta*, **457**, 133–170.
- Tirado-Rives, J. & Jorgensen, W. L. (1990). Molecular dynamics of proteins with the OPLS potential functions simulation of the third domain of silver pheasant ovomucoid in water. *J. Am. Chem. Soc.* **112**, 2773–2781.
- Treutlein, H. R., Lemmon, M. A., Engelman, D. M. & Brunger, A. T. (1992). The glycoporphin A transmembrane dimer: sequence-specific propensity for a right-handed supercoil of helices. *Biochemistry*, **31**, 12726–12732.

Edited by M. F. Moody

(Received 28 February 1997; received in revised form 20 June 1997; accepted 23 June 1997)